Development 133, 977-987 doi:10.1242/dev.02264

Inactivation of *Tbx1* in the pharyngeal endoderm results in 22q11DS malformations

Jelena S. Arnold[1], Uwe Werling[2], Evan M. Braunstein[1], Jun Liao[1], Sonja Nowotschin[1], Winfried Edelmann[2], Jean M. Hebert[1,3] and Bernice E. Morrow[1,*]

The 22q11 deletion (22q11DS; velo-cardio-facial syndrome/DiGeorge syndrome) is characterized by defects in the derivatives of the pharyngeal apparatus. Mouse genetic studies have identified *Tbx1*, a member of the T-box family of transcription factors, as being responsible for the physical malformations of the syndrome. Mice heterozygous for a null mutation in *Tbx1* have mild anomalies, whereas homozygous *Tbx1* mutants die at birth with severe defects in the derivatives of the pharyngeal apparatus, including cleft palate, thymus gland aplasia and cardiac outflow tract malformations. *Tbx1* is expressed in the splanchnic mesenchyme, the pharyngeal endoderm (PE) and in the core mesoderm of the pharyngeal apparatus. Tissue interactions between the epithelia and mesenchyme of the arches are required for development of the pharyngeal apparatus; the precise role of *Tbx1* in each tissue is not known. To assess the role of *Tbx1* in the PE, a conditional allele of *Tbx1* was generated using the Cre/loxP system. Foxg1-Cre was used to drive PE-specific ablation of *Tbx1*. Conditional null mutants survived embryogenesis, but died in the neonatal period with malformations identical to the defects observed in *Tbx1* homozygous null mutants. The abnormalities appear to be secondary to failed outgrowth of the pharyngeal pouches. These results show that *Tbx1* in the PE is required for the patterning and development of the pharyngeal apparatus, thereby disrupting the formation of its derivative structures.

KEY WORDS: *Tbx1*, Pharyngeal endoderm, Conditional inactivation

INTRODUCTION

22q11DS is the most common microdeletion syndrome in humans, occurring in 1/4000 live births (Burn and Goodship, 1996). Most patients have craniofacial anomalies, thymus gland hypoplasia or aplasia, hypocalcaemia and cardiac outflow tract defects (DiGeorge, 1965; Shprintzen et al., 1978). The affected tissues and organs derive from the pharyngeal apparatus, a transient embryonic structure lateral to the developing head. In mammalian species, the pharyngeal apparatus is segmented into five bilaterally symmetrical arches by the juxtaposition of the pharyngeal endoderm (PE) and ectodermal clefts. Neural crest cells (NCCs) migrate from the rhombomeres of the neural tube through the splanchnic mesenchyme to surround the core mesoderm of the pharyngeal arches (Bockman et al., 1989; Le Lievre and Le Douarin, 1975). Tissue interactions between the mesenchyme and the epithelia, including the cleft ectoderm and pouch endoderm, are required to form all of the derivatives of pharyngeal arches (Graham, 2003).

Numerous studies have emphasized the role of NCCs in the patterning of the pharyngeal arches (PAs). Classic ablation studies in chick have demonstrated that NCC removal results in abnormal development of the pharyngeal apparatus (Bockman et al., 1990; Kirby et al., 1983; Kirby and Waldo, 1990). More specifically, transplantation studies in chick embryos have shown that three different streams of NCCs migrate into the pharyngeal apparatus. Each stream provides the individual arches with a distinct identity (Noden, 1983). However, more recent experiments have demonstrated that individual arches can be formed and regionalized in the absence of NCCs (Veitch et al., 1999). Consequently, the role of all three germ layers in pharyngeal patterning has been reassessed, and it is now becoming clear that the PE may play a central role in the development of the pharyngeal apparatus. Part of its role may be in forming pouches, thereby segmenting the pharyngeal apparatus, while its other function may be in providing specific signals to surrounding tissues (Graham, 2003; Piotrowski et al., 2003; Piotrowski and Nusslein-Volhard, 2000). For example, it has been shown in chick embryos that NCCs respond to patterning cues produced by the PE, and that PE ablation at early developmental stages results in the loss of NCC-derived skeletal elements (Couly et al., 2002). However, most of the PE-specific signals required for patterning remain elusive.

Evidence pointing to the essential role of endodermal cells in patterning comes from *Tbx1* inactivation studies in the mouse. *TBX1*, a member of the T-box containing family of transcription factors, is the candidate gene most likely to be responsible for the pharyngeal arch-derived defects observed in individuals with 22q11DS (Jerome and Papaioannou, 2001; Lindsay and Baldini, 2001; Merscher et al., 2001). Throughout murine embryogenesis, *Tbx1* is expressed dynamically in multiple adjacent tissues relevant to the pharyngeal malformations in 22q11DS individuals. During early embryonic development (E8.5-E9.5) *Tbx1* is expressed in the splanchnic mesoderm ventral to the developing pharyngeal apparatus (Chapman et al., 1996). Later (E9.5-E11.5), *Tbx1* is expressed in both the PE and the core mesoderm (Chapman et al., 1996; Vitelli et al., 2002a; Yamagishi et al., 2003). However, *Tbx1* is not expressed in the NCC mesenchyme, despite the fact NCC ablation in the chick phenocopies the *Tbx1* homozygous null mutant phenotype (Bockman et al., 1990; Kirby et al., 1983; Kirby and Waldo, 1990). This suggests non cell-autonomous roles for the gene (Bockman and Kirby, 1989; Vitelli et al., 2002a; Xu et al., 2004).

Further support for indirect roles of *Tbx1* in NCC development derives from studies of *Tbx1* null mutations in mice. *Tbx1* heterozygous mutant mice survive in relatively normal Mendelian

[1]Department of Molecular Genetics, Albert Einstein College of Medicine, 1300 Morris Park Avenue, Bronx, NY 10461, USA. [2]Department of Cell Biology, Albert Einstein College of Medicine, 1300 Morris Park Avenue, Bronx, NY 10461, USA. [3]Department of Neuroscience, Albert Einstein College of Medicine, 1300 Morris Park Avenue, Bronx, NY 10461, USA.

*Author for correspondence (e-mail: morrow@aecom.yu.edu)

Accepted 28 December 2005

ratios, with mild cardiovascular defects and ectopic parathyroid glands (Jerome and Papaioannou, 2001; Liao et al., 2004; Lindsay and Baldini, 2001; Merscher et al., 2001). Homozygous null mutant mice (*Tbx1*$^{-/-}$) die in the perinatal period and have a severe pharyngeal phenotype (Funke et al., 2001; Jerome and Papaioannou, 2001; Liao et al., 2004; Lindsay and Baldini, 2001). PAs 2-6, fail to develop in *Tbx1*$^{-/-}$ embryos, leading to cleft palate, an absent outer and middle ear, thymus and parathyroid gland aplasia, aortic arch defects, a single cardiac outflow tract and ventricular septal defects (VSD). The phenotypic findings, together with the fact that *Tbx1* is not expressed in the NCCs, further support the view that the PE might be a key regulator of pharyngeal patterning.

However, because *Tbx1* is also expressed in the splanchnic mesenchyme and in the core mesoderm of the arches, the loss of pharyngeal patterning in the null mutants could be a result of *Tbx1* inactivation in the mesenchyme. To understand the role of *Tbx1* in the PE, we have inactivated *Tbx1* in the pharyngeal pouches by crossing Tbx1-floxed mice with the Foxg1-Cre mice (Hebert and McConnell, 2000; Pirvola et al., 2002). We demonstrate here that complete inactivation of *Tbx1* in the PE results in a phenotype identical to the *Tbx1* homozygous null mutant. We show that the phenotype is due to a failure in pharyngeal pouch outgrowth during the formation of the pharyngeal arches. Our experiments further strengthen the hypothesis that endodermal cells serve as a source of signals required for pharyngeal patterning and that *Tbx1* is a key regulator of this process.

MATERIALS AND METHODS

Tbx1 gene targeting

A 13 kb *Spe*I-*Eco*RV fragment containing *Tbx1* exon 1 through part of exon 6 was subcloned into the pZErO-2 plasmid (Invitrogen). A Hygromycin-resistance cassette, flanked by loxP sites, was inserted into the *Bst*BI site between exons 3 and 4. Oligonucleotides containing a single loxP site, flanked by *Ssp*I restriction sites were annealed, digested with *Ssp*I and inserted into the *Ssp*I site between exons 1 and 2. The linearized targeting vector (30 μg) was electroporated into 2.5×10^7 WW6 ES cells and cells were then selected for Hygromycin resistance. Colonies were picked after 10 days and their DNA was screened by PCR using the forward primer from the Hygromycin cassette, 5′-AGGTCCCTCGAAGAGGTTCA-3′, and reverse primer from exon 6, 5′-TACCACTGCCTCTCCAAATA-3′. Chimeric mice were generated by injecting C57BL/6 blastocysts with eight to twelve ES cells, derived from three separate ES clones. F1 animals were genotyped by PCR analysis with the forward primer from the Hygromycin cassette, 5′-AGGTCCCTCGAAGAGGTTCA-3′, and a reverse primer in the intronic region between exons 3 and 4, 5′-ACAAATAACCAGGCAC-TGGCA-3′. To delete the Hygromycin-resistance cassette and generate *Tbx1 flox*/+ mice, *Tbx1 hygro*/+ mice were crossed with lactate dehydrogenase-Cre (*Ldh1-Cre*) mice. The resulting offspring were genotyped with a forward primer in the *Tbx1* wild-type sequence, in the intronic region between exons 3 and 4, 5′-TGAAAAGCGGATCAAGGT-GC-3′, and with a primer spanning both the loxP site sequence and the *Tbx1* wild-type sequence immediately upstream of the Hygromycin cassette integration site, 5′-ATTTCCCTCGAATTCGGGCC-3′. In parallel, the offspring were screened for the deletion of the entire region between the single loxP site and the Hygromycin cassette, spanning exons 2 and 3, to generate *Tbx1 null*/+ mice. The forward primer used was proximal to the single loxP site, 5′-TCTTCTTGGGGCTGTAGACT-3′, whereas the reverse one was distal to the Hygromycin cassette integration site, 5′-ACAAATAACCAGGCACTGGCA-3′.

Mouse mutants and breeding

Tbx1 null/+ mice were backcrossed at least five generations into the Swiss Webster (SW) background and crossed with congenic SW *Foxg1-Cre*/+ mice to obtain compound heterozygotes (*Tbx1null/+;Foxg1-Cre*/+). To generate conditional mutants, these mice were subsequently crossed with *Tbx1 flox/flox* mice in the N3 C57BL/6 background. The Foxg1-Cre mice were genotyped as previously described (Hebert and McConnell, 2000). The congenic SW Foxg1-Cre mice were crossed to ROSA26 mice, congenic in the C57BL/6 background (Jackson Laboratories). The offspring heterozygous for both the Foxg1-Cre and ROSA26 alleles were dissected, stained with X-gal and genotyped as previously described (Hebert and McConnell, 2000).

Histology and bone/cartilage staining

Mouse embryos were dissected in phosphate-buffered saline (PBS), and fixed in 10% neutral-buffered formalin solution (Sigma) overnight. Following fixation, the embryos were dehydrated through graded ethanol, embedded in paraffin wax and sectioned (5-7 μm). All sections were stained with Hematoxylin and Eosin. Skeletal staining of E17.5 embryos was performed using Alcian Blue and Alizarin Red as previously described (Jerome and Papaioannou, 2001).

Whole-mount in situ hybridization

Digoxigenin-labeled RNA probes for *Tbx1* (Funke et al., 2001), *Myod*, *Fgf8* and *Fgf3* (cloned PCR fragment) were prepared by standard methods. Whole-mount and section in situ hybridization were performed as previously described (Epstein, 2000; Raft, 2004). Some *Tbx1*-hybridized embryos were embedded in agarose (3.5%, 8% sucrose, PBS) and vibratome sectioned at a thickness of 50 μm.

Immunohistochemistry

Tissue was prepared by 10% formaldehyde fixation of whole embryos, which were paraffin wax embedded and sectioned at a thickness of 10 μm. Affinity-purified rabbit anti-Tbx1 (Zymed) was diluted 1:100 in TBS/0.1% Triton X-100/5% goat serum/2% BSA, incubated for 1 hour at room temperature and detected with a biotinylated horse anti-mouse IgG conjugate (1:200; Vectalab), avidin-biotin complex formation (Vectalab) and DAB reaction (Research Genetics). Monoclonal 2H3 antibody was used as previously described (Raft, 2004).

RESULTS

To assess the importance of *Tbx1* in the pharyngeal pouches, we generated a conditional *Tbx1*-floxed allele harboring two loxP sites flanking exons 2 and 3 (Fig. 1A; ATG, exon 2). The resulting heterozygous *Tbx1 flox*/+ mice were generated by gene targeting and validated by genomic Southern blot hybridization (Fig. 1B) and PCR (Fig. 1C). In parallel, a null allele of *Tbx1* was generated by crossing *Tbx1 flox*/+ mice with βactin-Cre mice (Lewandoski et al., 1997) (Fig. 1). Heterozygous and homozygous null mutant mice appear similar to other null alleles that have been previously described (Jerome and Papaioannou, 2001; Liao et al., 2004; Lindsay and Baldini, 2001; Vitelli et al., 2003).

To inactivate *Tbx1* in the pharyngeal endoderm (PE), we used Foxg1-Cre mice. *Foxg1* drives expression of Cre recombinase in the telencephalon, the optic and otic vesicles, and in the PE (Fig. 2A,B) (Hebert and McConnell, 2000; Pirvola et al., 2002). The pattern of Foxg1-Cre-induced recombination was assessed using the ROSA26 reporter strain (Soriano, 1999). Consistent with the expression studies (Fig. 2A,B), recombination was evident in the pharyngeal pouches, the otic and optic vesicles, and the telencephalon (Fig. 2M-O).

Tbx1 flox/flox mice, which are viable and fertile (n=100), were crossed with *Tbx1 null/+; Foxg1-Cre*/+ mice to generate conditional null mutant mice. The resulting *Tbx1 flox/null; Foxg1-Cre*/+ conditional offspring are heterozygous for a *Tbx1* null allele in all tissues (*Tbx1 null*/+), but homozygous for the null allele in the PE and in the otic vesicle. *Tbx1* haploinsufficiency in adjacent tissues is not likely to affect the null mutant phenotype as most *Tbx1*$^{+/-}$ mice have a very mild pharyngeal phenotype (Jerome and Papaioannou, 2001; Liao et al., 2004; Lindsay and Baldini, 2001; Merscher et al., 2001). However, because Foxg1-Cre mice contain a knock-in mutation of Cre recombinase, the resulting conditional mutants also

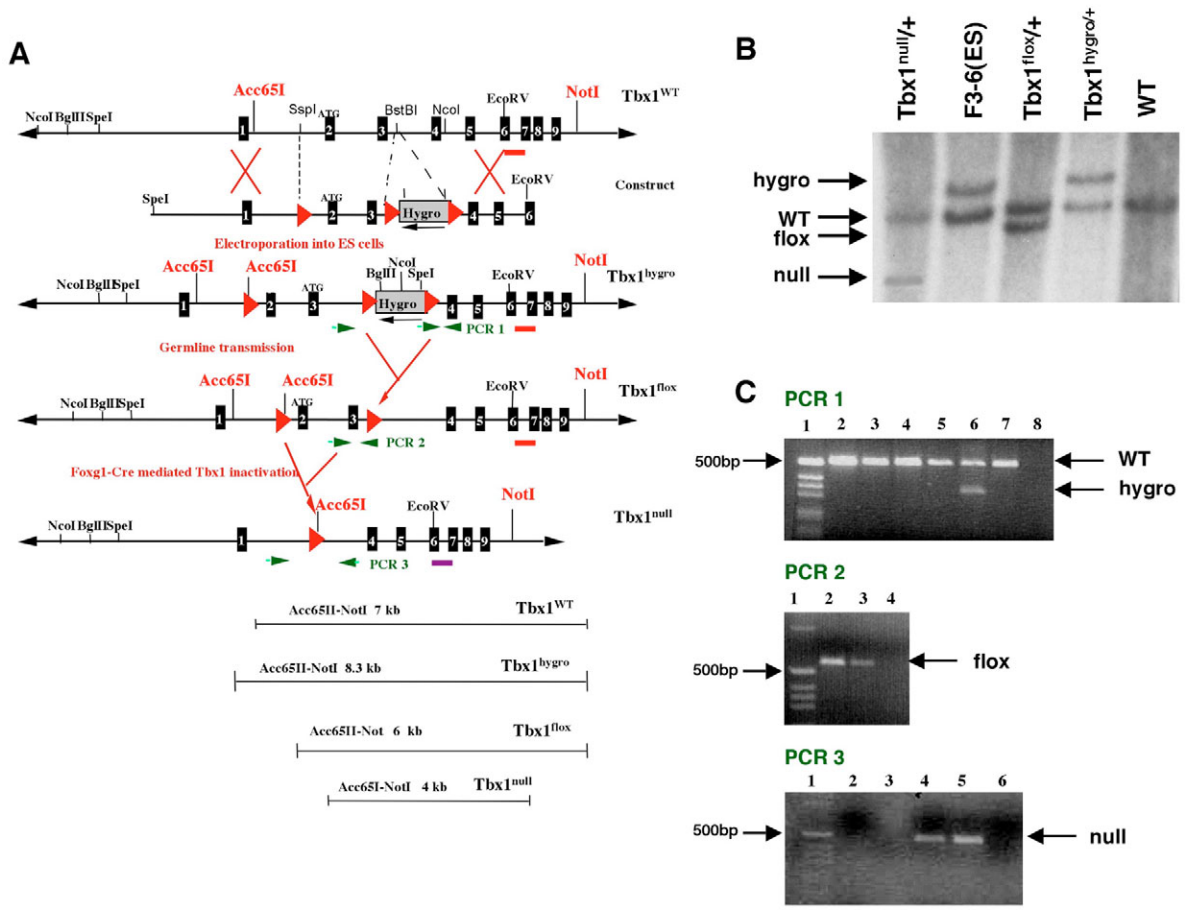

Fig. 1. Conditional inactivation strategy. (**A**) Generation of *Tbx1* wild-type (WT), *Tbx1* hygro, *Tbx1* flox and *Tbx1* null alleles. (**B**) Correct targeting was confirmed through Southern blot hybridization with a probe distal to the targeting vector integration site, indicated by the red bar in A. The restriction enzymes used were *Acc*65I and *Not*I, and the expected sizes of the different alleles are indicated in A. (**C**) PCR amplification was used to genotype the *Tbx1 hygro*/+ (lane 6; PCR1), *Tbx1 flox*/+ (lanes 2 and 3; PCR2) and *Tbx1 null*/+ (lanes 4 and 5; PCR3) mice. The position of the primers is indicated in A.

carry a null *Foxg1* allele. Fortunately, the *Foxg1* mutation is recessive (Hebert and McConnell, 2000; Tao and Lai, 1992) and *Tbx1*$^{+/-}$; *Foxg1-Cre*/+ double heterozygous embryos appear identical to the *Tbx1* single heterozygous mice, thus ruling out compound heterozygosity as a contributor to the mutant phenotype (n=20; data not shown). Additionally, we found that *Tbx1* expression is not altered in *Foxg1*$^{-/-}$ embryos and vice versa, suggesting that the two genes do not act in the same genetic pathway (see Fig. S1 in the supplementary material).

To diminish ectopic Cre activity, the conditional null mutant embryos were always generated as F1 offspring in the C56Bl/6/Swiss Webster genetic background (Hebert and McConnell, 2000). Tissue-specific inactivation of *Tbx1* in the *Foxg1* domain was determined by in situ hybridization (ISH) with a *Tbx1* probe. The pattern of expression in the conditional null mutants (Fig. 2E,F,H,J,L,Q,S,U) was compared with wild-type *Tbx1* expression (Fig. 2C,D,G,I,K,P,R,T) to ensure the conditional phenotype was due to loss of *Tbx1* in the PE. We found that *Tbx1* is expressed, as expected, in the mesoderm at E8.5 in both wild-type (Fig. 2C) and mutant (Fig. 2E) mice. At this stage, *Cre* mRNA is restricted to the prospective telencephalon (Fig. 2A). At E9.5, the conditional mutants show tissue-specific loss of *Tbx1* in the PE, while the splanchnic and core mesenchyme domain of expression remain intact (compare Fig. 2D,G with 2F,H). *Cre* mRNA expression (Fig. 2B) and Cre recombinase activity (Fig. 2M-O) at the same stage are evident in the forebrain, PE and otic vesicle. Immunohistochemistry with antiserum to the C-terminal third of Tbx1 protein, as well as radioactive ISH with *Tbx1* on sagittal histological sections, at E9.5 and E11.5, further confirm that expression in the splanchnic mesenchyme and the core mesoderm of the arches is intact in wild type (Fig. 2I,K,P,R,T) and conditional null mutants (Fig. 2J,L,Q,S,U).

To assess the impact of PE-specific inactivation of *Tbx1* on neonatal viability, Mendelian ratio analysis was performed on offspring from *Tbx1 null/+; Foxg1-Cre/+* and *Tbx1 flox/flox* crosses. *Tbx1 flox/null; Foxg1-Cre/+* did not survive beyond the neonatal period (n>100), indicating that *Tbx1* in the PE is required for survival. Both conditional null mutants and *Tbx1*$^{-/-}$ embryos are present in normal Mendelian ratios at E17.5, demonstrating that they survive embryogenesis.

Tbx1 in the PE is required for development of the distal pharyngeal apparatus

Conditional null mutant embryos were dissected at E11.5 to analyze development of the pharyngeal apparatus. In comparison with wild-type littermates, which show clear segmentation of all

pharyngeal arches (Fig. 3A), only PA1 is present in conditional null mutant embryos (Fig. 3B). Coronal sections through the same embryos confirmed the presence of a hypoplastic pharynx in the conditional null embryo, lacking distinct distal arches (3D). As compared with wild-type embryos, the first pouch appears to be hypoplastic in the mutants, while the distal pouches do not form (Fig. 3D). The lack of caudal pouch segmentation and the loss of PE-specific gene expression were also assessed with molecular markers. Both *Fgf3* and *Fgf8* are expressed in the pharyngeal pouches at E10.0 (Fig. 4A,C). However, stage-matched conditional null mutants show loss of both Fgf genes in the pharyngeal pouches (Fig. 4B,D). Conversely, *Fgf8* expression in the pharyngeal ectoderm is unaffected in the conditional null mutants.

Inactivation of *Tbx1* in the PE results in failed development of the craniofacial skeleton and musculature

Conditional null mutant embryos at E17.5 are edematous (Fig. 5B and data not shown) when compared with wild-type embryos (Fig. 5A), and appear smaller. They have an abnormal facial structure and absent external and middle ears (Fig. 5B and data not shown). Both the outer ear and the middle ear ossicles develop as a result of epithelial-mesenchymal tissue interactions (Fekete and Wu, 2002; Lindsay and Baldini, 2001), which are disrupted by *Tbx1* inactivation in the PE.

In addition to ear defects, all conditional mutant embryos analyzed (n=10 at E17.5) have craniofacial abnormalities, including cleft palate (Fig. 5D). Bone and cartilage staining revealed facial

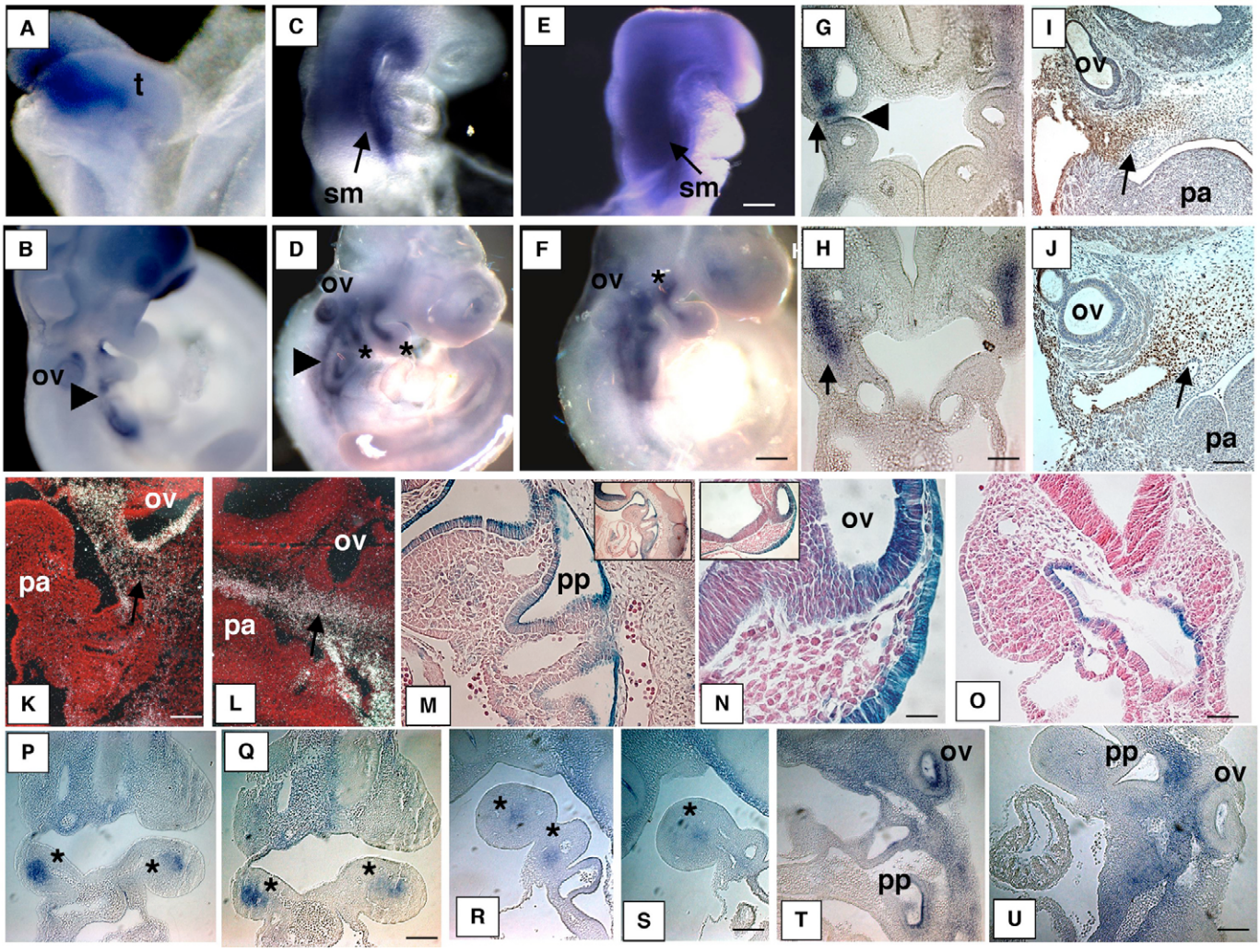

Fig. 2. *Tbx1* expression compared with Cre expression. *Tbx1* expression in wild-type (**C**,**D**,**G**,**I**,**K**) and homozygous conditional mutant mice (**E**,**F**,**H**,**J**,**L**) at E8.5 (C,E) and E9.5 (D,F-H), compared with Cre expression in Foxg1-Cre mice at E8.5 (**A**) and E9.5 (**B**). Coronal vibratome sections of whole mounts from D (wild type) and F (mutant) are shown in G and H, respectively. Note *Tbx1* expression in the core mesenchyme (arrows) of both wild-type (G) and mutant embryos (H). The wild type also shows expression in the pharyngeal pouch endoderm (arrowhead in G). Immunohistochemistry with a polyclonal Tbx1 antibody on E11.5 sagittal sections confirms the presence of the Tbx1 protein in the splanchnic mesenchyme (arrow) of the mutant (J) and wild-type (I) embryos. Radioactive ISH on E11.5 sagittal sections shows *Tbx1* expression in the otic vesicle (ov) and the adjacent splanchnic mesenchyme (K). The OV expression of *Tbx1* is absent from the conditional null embryo (L), although the mesenchymal staining remains intact. (**M-O**) X-gal staining of E9.0 (O) and E9.5 (M,N) sagittal (M) and transverse (N,O) sections of ROSA26/Foxg1-Cre progeny. Cre activity is evident in the pharyngeal pouches (pp) and the otic vesicle (ov). (**P-U**) *Tbx1* expression by ISH on coronal (P,Q) and sagittal (R-U) sections in control (P,R,T) and conditional null embryos (Q,S,U). Scale bars: 100 μm in E,H,N,Q,S,U; 0.2 mm in F; 0.5 mm in J,K. Asterisks indicate core mesoderm; ov, otic vesicle; pa, pharyngeal arch; pp, pharyngeal pouches.

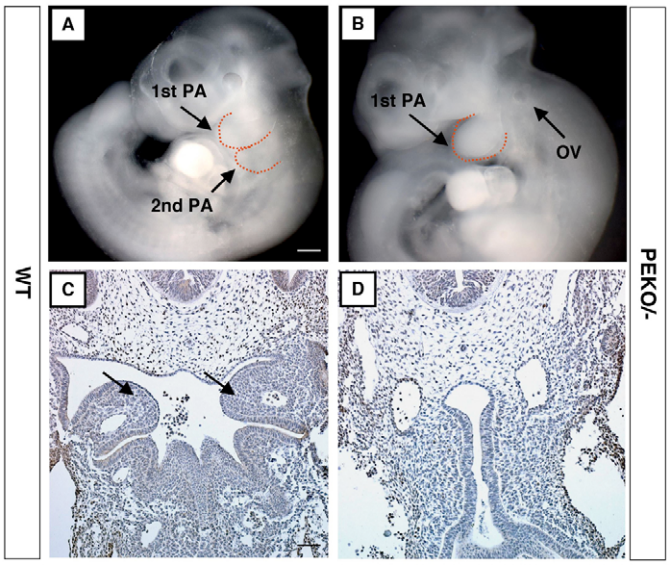

Fig. 3. The *Tbx1* conditional mutant phenotype. (**A**,**B**) *Tbx1* conditional mutant phenotype at E11.5 (B) compared with a wild-type littermate (A). PAs are indicated with a dashed red line and denoted with arrows. PA, pharyngeal arch. (**C**,**D**) Coronal sections through the same embryos show a hypoplastic pharynx in the mutant (D) compared with the wild-type littermate (C). PEKO/–, *Tbx1 flox/null; Foxg1-Cre*/+; WT, wild type. Scale bars: 0.5 mm in A; 300 μm in C.

bone defects, including hypoplasia of the temporal and hyoid bones, absence of the zygomatic arch and the tympanic ring, and fusion of the basioccipital and basisphenoid bones (Fig. 5F,H; data not shown). The mandible of the mutants is shorter than that of wild type and the coronoid process is missing (data not shown). None of the conditional heterozygous mutants analyzed (n=30) display craniofacial defects (data not shown). This indicates that complete inactivation in the PE is required to obtain the observed malformations.

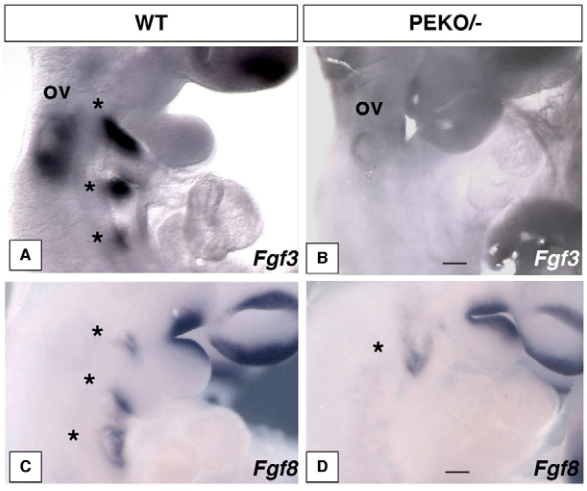

Fig. 4. ISH with *Fgf3* and *Fgf8*. (**A-D**) ISH with *Fgf3* (A,B) and *Fgf8* (C,D) probes at E10.0 reveals expression of both genes in the pharyngeal pouches (asterisks) of wild-type embryos (A,C). Conditional null embryos of the same stage (B,D) display a loss of both *Fgf3* and *Fgf8* in the pharyngeal pouches. OV, otic vesicle; PEKO/–, *Tbx1 flox/null; Foxg1-Cre*/+; WT, wild type. Scale bars: 0.1 mm.

Conditional inactivation of *Tbx1* also affects two of the muscles of mastication, derived from PA1. When compared with wild-type embryos (Fig. 6A,C), the masseter and pterygoid muscles are either absent or severely hypoplastic in mutant embryos (Fig. 6B,D). Likewise, PA1-derived craniofacial muscles are also missing in *Tbx1*$^{-/-}$ embryos (Kelly et al., 2004; Liao et al., 2004). By contrast, E17.5 Tbx1 hygro/hygro embryos (see Materials and methods), which are severely hypomorphic for *Tbx1* expression (10% of wild-type levels, determined by quantitative RT-PCR, see Fig. S2 in the supplementary material) and have abnormal craniofacial bone structure, show normal development of the facial muscles (masseter; Fig. 6E,F). This shows that the muscle defects are not secondary to skeletal bone malformations. It also suggests that skeletal muscle development is not highly sensitive to *Tbx1* gene dosage but relies instead on correct spatial and temporal expression of the gene. PA2 in both the null and conditional *Tbx1* embryos is hypoplastic or missing, and the

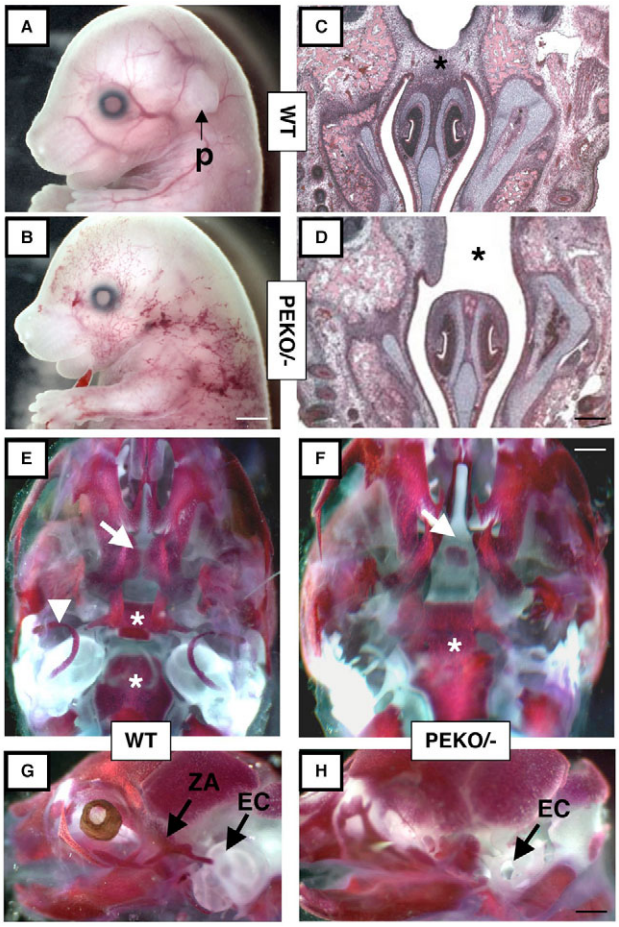

Fig. 5. Craniofacial phenotype of *Tbx1* mutants at E17.5, shown by transverse histological sections, and bone and cartilage staining. (**A**) Wild-type embryo. (**B**) The conditional mutant embryos at E17.5 are edematous and lack the pinna (p). (**C**,**D**) Histological analysis of the mutant (D) compared with wild-type offspring (C) reveals the presence of cleft palate in the mutants (D, star). (**E-H**) Bone and cartilage staining of E17.5 wild-type (E,G) and mutant (F,H) embryos. The mutant (F) has cleft palate (arrow), aplasia of the tympanic rings (arrowhead in E), and fused basisphenoid and basioccipital bones (asterisks). EC, ear capsule; PEKO/–, *Tbx1 flox/null; Foxg1-Cre*/+; WT, wild type; ZA, zygomatic arches. Scale bars: 0.8 mm in B; 300 μm in D; 0.5 mm in F,H.

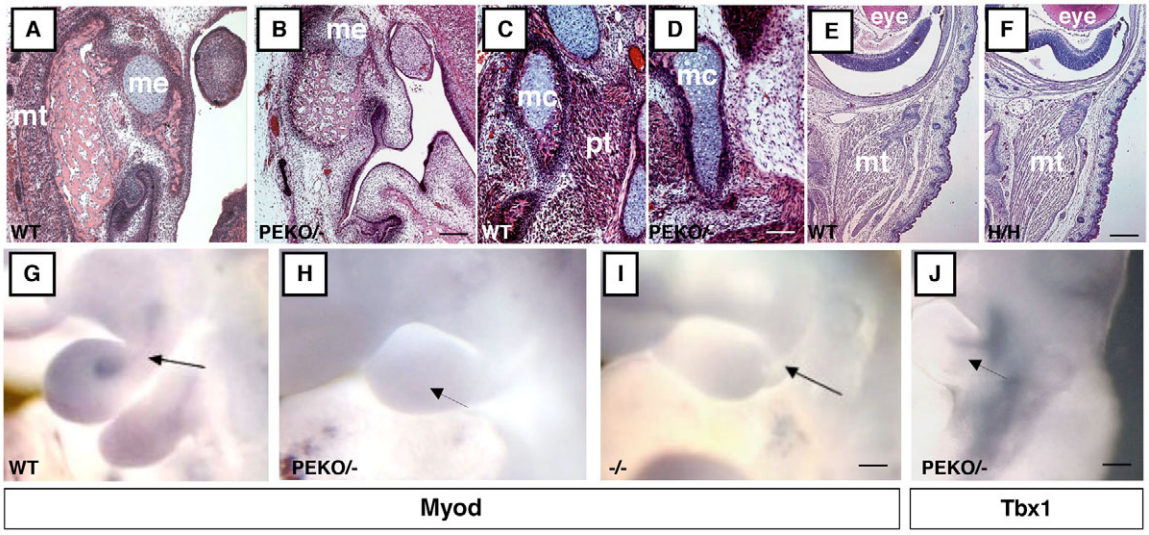

Fig. 6. *Tbx1* conditional null embryos have abnormal musculature. (**A-D**) Transverse histological sections of E17.5 embryos. *Tbx1* conditional null embryos have hypoplasia of the masseter (B) and pterygoid (D) muscles. Representative wild-type embryos are shown in A and C. mc, mandibular condyle; me, Meckel's cartilage; mt, masseter; pt, pterygoid. (**E**,**F**) Coronal sections through an E17.5 Tbx1 hygro/hygro embryo (H/H; F) reveal the presence of the masseter muscle (mt); a wild-type control embryo is shown in E. (**G**) ISH with *Myod* on an E10.5 wild-type embryo shows expression in the core mesenchyme of PAs (arrow). (**H**,**I**) *Myod* ISH reveals the lack of expression in the core mesenchyme of the first PA of homozygous conditional null (H) and *Tbx1*$^{-/-}$ (I) embryos. (**J**) *Tbx1* expression in the core mesenchyme of PA1 is maintained in the homozygous conditional null mutant at E10.5 (arrow). WT, wild type; PEKO/–, *Tbx1 flox/null; Foxg1-Cre/+*; –/–, *Tbx1*$^{-/-}$. Scale bar: 100 μm in B,D; 200 μm in F; 0.5 mm in I; 0.2 mm in J.

resulting muscles do not form (Kelly et al., 2004). As above, conditional heterozygote animals have normal craniofacial muscles (data not shown).

The core mesoderm of the pharyngeal arches is populated by cranial paraxial mesoderm cells giving rise to branchiomeric skeletal muscles of the head and neck, including the muscles of mastication (Couly et al., 1992; Noden, 1983; Trainor et al., 1994). Members of the Myod family of basic HLH myogenic factors have been shown to specify skeletal muscle lineages throughout the embryo (Buckingham, 2001). To determine the basis for abnormal skeletal muscle development in *Tbx1* conditional mutants, *Myod* expression was assessed by whole-mount ISH at E10.5 (Fig. 6G-J). *Myod* is normally activated in PA1-2 of wild-type embryos (Fig. 6G); however, in conditional null mutants (Fig. 6H) and in *Tbx1*$^{-/-}$ embryos (Fig. 6I) *Myod* is not expressed in PA1 (n=3). To assess mesenchymal cell specification in PA1, capsulin (*Tcf21* – Mouse Genome Informatics) expression was analyzed in *Tbx1* conditional and null mutants at E10.5. A normal expression pattern of capsulin transcripts was observed in the PA1 core mesoderm in conditional (data not shown) and null *Tbx1* mutants at E10.5 (Kelly et al., 2004). Importantly, *Tbx1* is expressed in the core mesoderm of PA1 in conditional null mutants (see Fig. 2K, Fig. 6J). Failure to activate *Myod* in conditional mutant embryos in the presence of at least some *Tbx1* expression in the core mesoderm suggests a non cell-autonomous role for the gene in the morphogenesis of the derivatives of PA1.

Tbx1 in the PE is required for the development of the thymus and parathyroid glands

The thymus, thyroid and parathyroid glands, derived from pharyngeal pouches, are absent in *Tbx1*$^{-/-}$ embryos. Conditional null embryos at E17.5 lack thymus and parathyroid glands, whereas the thyroid glands are smaller and ectopically located (compare Fig. 7A,C with 7B,D). By contrast, all *Tbx1* conditional heterozygous embryos examined (n=30) have normal thymus and thyroid gland morphology, although the parathyroid glands are ectopically placed (data not shown). The defects observed in conditional null embryos are a result of a failure of the formation of the distal pharyngeal pouches required to form these glands.

Cardiovascular defects in conditional null mutants

Cardiovascular defects, including malformations of the aortic arch and conotruncal (outflow tract) heart defects, occur in 60-75% of individuals with 22q11DS (Momma et al., 1996). All conditional null mutants analyzed have aortic arch defects, including retroesophageal right subclavian artery (RSA). Compared with wild-type littermates, which show the normal location of the right subclavian artery (Fig. 7A), all conditional null mutants analyzed have an RSA, a condition in which this artery originates anomalously from the aortic arch and passes dorsal to the esophagus and the trachea (Fig. 7B). In addition, all conditional null mutants have conotruncal heart defects. The outflow tract (OFT), which connects the pharyngeal arch arteries with the developing heart, becomes remodeled during embryonic development to form the ascending aorta and pulmonary trunk. The resulting separation of the systemic and pulmonary circulation is evident in wild-type embryos at E17.5 (Fig. 7E). However, all conditional null embryos analyzed at E17.5 have a single OFT, a malformation known as persistent truncus arteriosus (PTA) (Fig. 7F). The most proximal part of the OFT, the conal septum, which normally contributes to the closure of the interventricular (IV) septum, is also affected in both *Tbx1* null (Fig. 7I) and conditional mutants (Fig. 7H). In these mice, the single arterial orifice is connected exclusively to the right ventricle, whereas the left ventricle communicates with the right one through a large ventricular septal defect (VSD) (Fig. 7H). Interestingly, a VSD has also been previously detected in haploinsufficient (Df1/+) and overexpressing mouse models of *Tbx1* (BAC 316.23) with normal

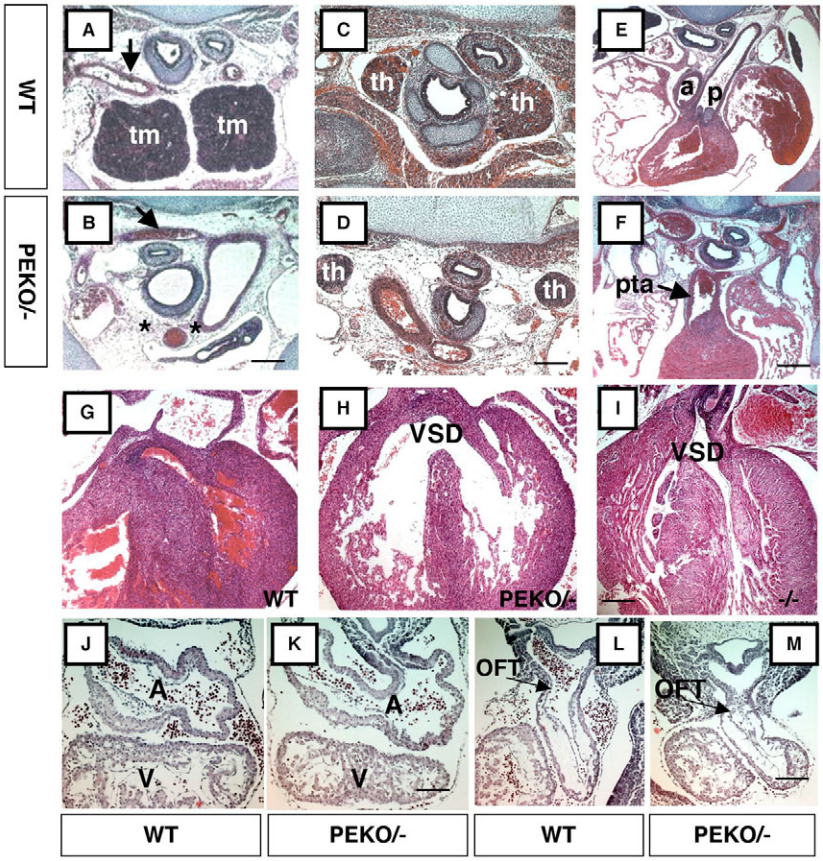

Fig. 7. Thymus, thyroid and cardiovascular phenotype of *Tbx1* conditional mutants shown by transverse histological sections. (**A**) An E17.5 wild-type embryo with the thymus gland (tm) and the location of the right subclavian artery (arrow) indicated. (**B**) A homozygous conditional null embryo of the same stage shows thymus aplasia (asterisks), as well as the presence of a retroesophageal right subclavian artery (RSA, arrow). (**C**,**D**) The thyroid glands (th) of wild-type (C) and mutant (D) embryos at E17.5. (**E**) Wild-type embryo shows normal separation of the aortic (a) and pulmonary (p) trunks. (**F**) Abnormal septation of the outflow tract results in persistent truncus arteriosus (PTA) in the mutant of the same stage. (**G-I**) Sections through the heart show a ventricular septal defect (VSD) in a *Tbx1* homozygous conditional mutant (H) and a $Tbx1^{-/-}$ embryo (I), compared with a wild-type litter mate (G). (**J-M**) Transverse sections at E10.5 show normal development of atria (A) and ventricles (V), as well as the outflow tract in both wild-type (J,L) and conditional mutant (K,M) embryos. WT, wild type; PEKO/–, *Tbx1 flox/null; Foxg1-Cre*/+; –/–, $Tbx1^{-/-}$. Scale bars: 300 μm in B,D,F; 100 μm in G-I; 50 μm in K,M.

pharyngeal arch development (Merscher et al., 2001; Vitelli et al., 2002a), indicating that OFT defects can arise independently of PA patterning defects.

Tbx1 null embryos have been shown to display PTA not only due to NCC migration defects but also due to hypoplasia of the distal OFT myocardium (Xu et al., 2004). In order to assess whether OFT defects observed in conditional null embryos arise from a loss of myocardial progenitors arising from the secondary heart field during early embryogenesis, *Tbx1 flox/null; Foxg1-Cre*/+ embryos were analyzed at E10.5 for cardiovascular defects. All of the E10.5 mutant embryos analyzed (n=5) display hypoplasia of the distal OFT, indicating that inactivation of *Tbx1* in the PE also affects elongation of the OFT from cells of the secondary heart field (Fig. 7J-M).

Conditional heterozygous mice survive in normal Mendelian ratios (55/115, 48%), in contrast to the $Tbx1^{+/-}$ mice, which have a 10% incidence of neonatal lethality (Vitelli et al., 2002a; Xu et al., 2004). Because previous studies have shown that 10-30% of $Tbx1^{+/-}$ mice have RSA (Fig. 8C) and, occasionally, Tetralogy of Fallot (TOF) or double outlet right ventricle (DORV) (Liao et al., 2004; Lindsay and Baldini, 2001), *Tbx1* conditional heterozygous mice were analyzed for the presence of these malformations. The PAAs in the conditional heterozygous embryos (n=30) are normal at E10.0 (Fig. 8B), in contrast to the fourth PAA aplasia observed in 10-100% of $Tbx1^{+/-}$ embryos, depending on the genetic background analyzed (Liao et al., 2004; Lindsay and Baldini, 2001; Vitelli et al., 2002a). However, the presence of normal fourth PAAs in these embryos does not exclude the possibility of a later aortic arch phenotype due to abnormal regression of the embryonic arteries. To assess the remodeling of the PAAs, conditional heterozygous embryos were analyzed at E17.5 by histological sections. None of the E17.5 conditional heterozygous embryos examined (n=30) have any

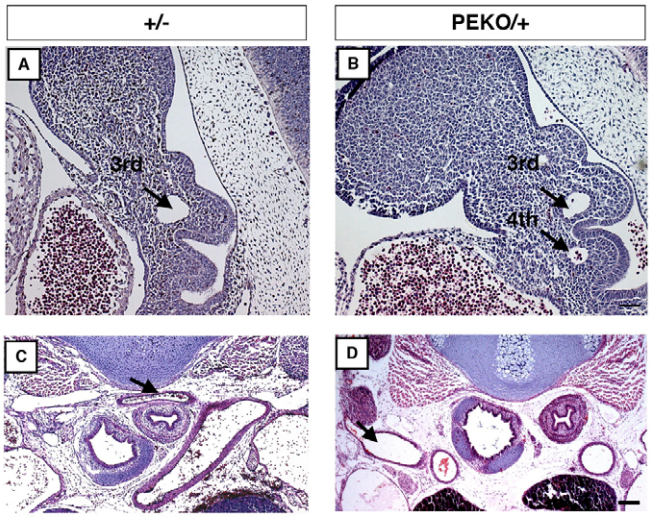

Fig. 8. *Tbx1* heterozygous conditional phenotype. (**A**) $Tbx1^{+/-}$ mice have aplasia of the left fourth pharyngeal arch artery (PAA), as shown by sagittal histological sections at E10.5 (arrow indicates third PAA). (**B**) Conditional heterozygous mice appear normal at the same stage, with both the third and fourth PAA clearly present (arrows). (**C**,**D**) E17.5 $Tbx1^{+/-}$ embryos have RSA (arrow in C), whereas all conditional heterozygotes appear normal (D). The right subclavian artery in the conditional mutant (D) is indicated with an arrow. +/–, $Tbx1^{+/-}$; PEKO/+, *Tbx1 flox*/+; *Foxg1-Cre*/+. Scale bars: 200 μm in B,D.

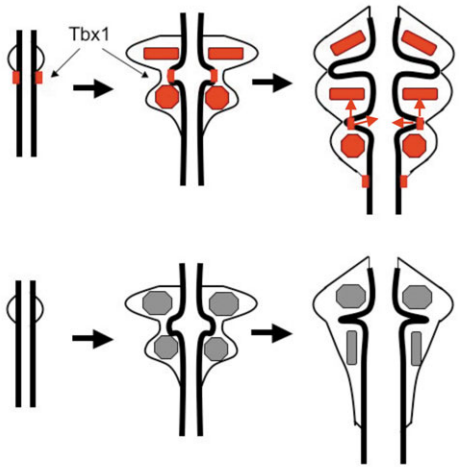

Fig. 9. Model of *Tbx1* function in pharyngeal development (E9.5-E11.5). (Top) In wild type, pharyngeal arches develop as bulges on either side of the pharyngeal endoderm (bold lines, coronal section; rostral, top; caudal, bottom). The arrows indicate approximate time in development; left, earliest, right, latest times. *Tbx1*, shown as red boxes on the endodermal lining, marks the position of the future pharyngeal pouches, which will extend outward to meet the surface ectodermal clefts. *Tbx1* is expressed in the PE during pouch outgrowth but becomes downregulated once the pouches form. The gene is also expressed in the core mesenchyme of the developing arches, indicated by red boxes and circles. It is likely that *Tbx1* in the endoderm is involved in epithelial-mesenchymal interactions with the core mesoderm (red arrows). (Bottom) Lack of distal pouch development in $Tbx1^{-/-}$ and conditional null embryos prevents the segmentation of the distal apparatus, altering NCC migration, growth and differentiation.

noticeable abnormalities of the aortic arch or outflow tract (Fig. 8D). This observation underscores important differences between the $Tbx1^{+/-}$ and the conditional heterozygous allele in the PE domain of expression, and suggests that *Tbx1* in the core mesoderm perhaps has essential roles in forming the fourth PAAs.

DISCUSSION

Tbx1 in the development of the pharyngeal pouches

In this report, we show that inactivation of *Tbx1* in the endoderm of the pharyngeal apparatus sets off a chain of events leading to malformations in the derivatives of this structure that are identical to those in the $Tbx1^{-/-}$ mutant. A model has been generated to illustrate the events resulting in the observed congenital anomalies (Fig. 9). In this model, *Tbx1*, expressed in the PE, is required for the formation of pouches. Once pouches fail to form, the first notable defect in these mutants, tissue interactions are disrupted, thereby preventing neural crest cells (NCCs) from entering and developing into their derivative structures.

This model is derived from the observed phenotype in the conditional null mutant mice and from previous mouse genetic studies (Vitelli et al., 2002a; Xu et al., 2004; Yamagishi et al., 2003), as well as from embryological experiments (Bockman and Kirby, 1989; Clouthier et al., 2000; Crump et al., 2004; Graham, 2003; Kirby et al., 1983). It has been suggested that in the absence of *Tbx1*, NCCs leave the neural tube but fail to populate the unsegmented distal pharyngeal apparatus completely, resulting in a hypoplastic distal pharyngeal region (Fig. 3) (Jerome and Papaioannou, 2001; Liao et al., 2004; Vitelli et al., 2002a). However, it remains unclear whether this defect is primary to the function of *Tbx1* in the PE, or secondary to its expression domains in the splanchnic mesenchyme or core mesoderm of the pharyngeal arches. The results of this study, in which *Tbx1* was specifically inactivated in the PE, demonstrate the essential function of *Tbx1* in the PE during the formation of the derivatives of the pharyngeal apparatus.

The findings in this report are further supported by studies of a zebrafish *tbx1* hypomorphic mutant termed *van gogh* (*vgo*). As in the *Tbx1* null mutant mouse embryo, the distal pharyngeal apparatus fails to develop in *vgo* mutants (Piotrowski et al., 2003; Piotrowski and Nusslein-Volhard, 2000). As expected, expression of zebrafish *tbx1* correlates with murine *Tbx1* (Chapman et al., 1996; Piotrowski et al., 2003; Vitelli et al., 2002a). Furthermore, the *vgo* study showed that transplantation of endodermal cells from wild-type embryos rescued cartilage malformations in homozygous zebrafish *vgo* mutants. These results suggest that cartilage defects in homozygous *vgo* mutants result from defective signaling from the pharyngeal endoderm (Piotrowski et al., 2003). Finally, NCC induction and migration appeared normal in *vgo* mutants, indicating that abnormal skeletal development in the mutants is not due to a primary NCC defect (Piotrowski et al., 2003) and that the endoderm is the source of a secreted signal required for the proper differentiation of NCC-derived mesenchyme (Fig. 9).

Tbx1/*Fgf8* interaction may be required for PE development

Further evidence for the importance of the PE in the development of the pharyngeal apparatus and its derivatives comes from studies of *Fgf8*, a secreted fibroblast growth factor expressed in the pharyngeal endoderm, ectoderm and mesoderm (Hu et al., 2004; Lewandoski et al., 1997; Meyers et al., 1998). Homozygous *Fgf8* hypomorphic (*Fgf8 neo/–*) and conditional mutant embryos, in which expression is downregulated either in the ectoderm alone or in both the ectoderm and the PE, have a closely related phenotype to that of $Tbx1^{-/-}$ embryos and the conditional null mutants (Abu-Issa et al., 2002; Frank et al., 2002; Macatee et al., 2003). In addition, mice heterozygous for both *Tbx1* and *Fgf8* have a higher penetrance of aortic arch defects than do $Tbx1^{+/-}$ mice alone as a result of an increased severity of fourth PAA defects (Vitelli et al., 2002b). Finally, *Fgf8* is downregulated in the pharyngeal pouches of both $Tbx1^{-/-}$ and conditional null embryos (Fig. 8). This suggests a functional connection between *Tbx1* and *Fgf8* in the PE. The interactions between the two genes might be therefore responsible for inducing a developmental program necessary for the proper patterning of the pharyngeal apparatus (arrows, Fig. 9).

Role of *Tbx1* in pharyngeal pouch outgrowth

There are multiple explanations for the failure of pharyngeal pouch outgrowth when *Tbx1* is inactivated in the PE. Some possibilities are reduced cell proliferation, increased apoptosis or migration defects. A recent report has provided direct evidence for the role of *Tbx1* in the proliferation of PE cells at sites of pharyngeal pouch outgrowth (Xu et al., 2005). The study used an inducible, Tamoxifen-responsive Cre line (TgCAGG-CreER^{TM}) to inactivate *Tbx1* immediately following the formation of pharyngeal pouches. Results of this study showed a 50% reduction in the number of proliferating PE cells in the newly formed distal PAs. Conversely, no changes were detected in the proliferation of pharyngeal mesenchyme cells. It is likely that the same mechanism is responsible for the failure of distal PP formation in the conditional null mutants.

Alternatively, it is possible that increased apoptosis could be responsible for the failure of the formation of distal pouches. Increased programmed cell death has been observed in the pharyngeal pouches of *Fgf8* hypomorphic mice (*Fgf8 neo/–*), which contain one null allele of the gene and exhibit a phenotype related to that of *Tbx1*$^{-/-}$ embryos (Abu-Issa et al., 2002; Xu et al., 2005). Analysis of *Fgf8 neo/–* embryos revealed areas of increased cell death overlapping with *Fgf8* expression, as well as in the NCCs (Abu-Issa et al., 2002). *Fgf8* is not expressed in the NCCs, suggesting that PE and ectodermal cells expressing the gene might be required to maintain survival of the NCCs, and that *Tbx1* in the PE could in turn regulate this process (Abu-Issa et al., 2002). The third possibility is that the PE cells fail to migrate properly when *Tbx1* is inactivated. The pouch endoderm proliferates on a proximodistal axis and migrates towards the invaginating ectoderm, thus providing physical segmentation of the individual arches (Graham and Smith, 2001). Recent experiments link actin cables within endodermal cells, via N-cadherin and adherens junctions, to pharyngeal pouch outgrowth in the chick (Quinlan et al., 2004). It is possible that *Tbx1* may play a role in shaping the pouches as well.

Reduced *Tbx1* expression in the PE is not sufficient to produce aortic arch defects

Inactivation of one *Tbx1* allele is sufficient to produce mild but consistent defects. *Tbx1*$^{+/-}$ mice show neonatal lethality with reduced penetrance due to cardiovascular defects resulting from fourth PAA aplasia (Lindsay and Baldini, 2001; Merscher et al., 2001b; Vitelli et al., 2002a). In contrast to *Tbx1*$^{+/-}$ mice, inactivation of one *Tbx1* allele specifically in the PE does not affect survival (n=115). Furthermore, the conditional heterozygotes do not exhibit the detectable fourth PAA or aortic arch malformations (n=30) that are observed in *Tbx1*$^{+/-}$ mice. This suggests that other domains of *Tbx1* expression, possibly the core mesoderm, contribute significantly to fourth PAA formation, growth and remodeling. It is also known that the core mesoderm participates in forming the endothelial layer of the PAA vessels (Kirby and Waldo, 1995). Another possible explanation for the discrepancy between the severity of the homozygous and heterozygous conditional phenotype and that of the null mice could be that the expressivity of the heterozygous phenotype is affected by genetic background differences.

Tbx1 in the PE is required for cardiac outflow tract septation

Conditional inactivation of *Tbx1* underlies the crucial role of the gene in the PE in cardiac OFT septation. Whereas the heart myocardium derives from lateral plate mesoderm precursors (the primary heart field), the OFT myocardium derives from the splanchnic mesoderm located caudal to the pharynx (the secondary heart field, or SHF) (Kelly and Buckingham, 2002). In addition, NCCs migrate to populate the AP septum and participate in the remodeling of the OFT. The phenotype of the conditional null mutants, together with the fact that *Tbx1* is not expressed in the NCCs, suggests that endodermal *Tbx1* plays an important role in OFT development. *Tbx1* in the PE most likely regulates both NCC migration into the AP septum and the elongation of the OFT from the SHF, as early morphogenesis of the OFT is affected in conditional null mutants. A recent study reported *Tbx1* expression in the endodermal lining of the aortic sac, providing a regional correlation with the morphogenetic defect (Xu et al., 2004). Alternatively, the AP septum abnormality could be secondary to reduced NCC migration through the fourth PAA. PTA, a result of abnormal OFT septation, also leads to VSD, as the IV septum cannot fuse with the abnormal AP septum. The VSD observed in *Tbx1* conditional embryos could therefore be a secondary effect resulting from OFT septation defects.

A second role for *Tbx1* in the PE has been proposed. A recent report showed that even in the presence of pharyngeal pouch outgrowth failure, low levels of *Tbx1* can rescue OFT alignment defects, which lead to VSD in *Tbx1*$^{-/-}$ mice (Xu et al., 2004). Furthermore, the study used the Nkx2.5-Cre strain to inactivate *Tbx1* in the SHF, as well as in the caudal pharyngeal pouches. Conditional mutants showed the presence of OFT defects even when PE segmentation into pouches was unaffected, probably because *Tbx1* was inactivated later in development than it was by Foxg1-Cre, suggesting that *Tbx1* has another distinct role in the alignment of OFT.

Non cell-autonomous role of *Tbx1* in the development of the core mesoderm

The muscles of mastication, derived from PA1 (Hacker and Guthrie, 1998), are missing in *Tbx1* null mutant embryos and, more importantly, in the PE-specific conditional null mutants. The NCC mesenchymal cells lie between the PE and the core mesoderm. We show that two Fgf ligand genes, *Fgf3* and *Fgf8* are downstream of *Tbx1* in the PE. Abnormal myogenesis, together with the finding that core mesoderm cells are present in conditional null mutants, suggests that signaling between the NCCs and the PE, perhaps via *Fgf3* and *Fgf8*, disrupts the development of the core mesoderm and that this process is independent of the expression domain of *Tbx1* in the core mesoderm.

In addition to the PE expression, the mesodermal *Tbx1* domain could also act as a source of signaling molecules mediating the patterning and segmentation of the pharyngeal apparatus. Other Fgf genes could mediate these signals, possibly *Fgf10*, in the core mesoderm. Previous studies have already shown that *Fgf10* is a direct downstream target of *Tbx1*, and, as such, it could be involved in relaying core mesoderm-derived signals to the adjacent NCCs and to the PE (Xu et al., 2004). Furthermore, a recent zebrafish study found that cells expressing *Fgf8* and *Fgf3* are required to promote pouch formation, and proposed a model in which Fgf signaling in the mesoderm and segmented hindbrain organizes the development of the PE into distinct pouches (Crump et al., 2004). Tissue-specific ablation of *Tbx1* in the core mesoderm will be necessary to address this question.

In summary, conditional inactivation of *Tbx1* in the PE demonstrates an early cell-autonomous role for the gene in the patterning and outgrowth of the pharyngeal pouches. Lack of segmentation of the pharyngeal apparatus indirectly causes the myriad of NCC mesenchyme-mediated malformations in the derivatives of the pharyngeal apparatus. Analysis of the conditional mutants supports the emerging model of the PE as a source of the inductive signals that are necessary for proper development of the pharyngeal apparatus and its derivatives. Inactivation of *Tbx1* in the PE is likely to affect core mesoderm development as well, resulting in the failed development of the muscles of mastication. Furthermore, development of the fourth PAA and its remodeling is not dependent solely on the PE but requires input from other *Tbx1* expression domains, possibly the core mesoderm. Finally, our study contributes not only to the

understanding of pharyngeal arch formation and remodeling, but also to the identification of novel mechanisms responsible for the pathogenesis of 22q11DS.

Note added in proof

Depending on the genetic background, the Foxg1-Cre mouse line can also mediate recombination in the core mesoderm of the pharyngeal arches (Zhang et al., 2005). To maintain Cre expression restricted to the pharyngeal endoderm, we used the Foxg1-Cre line congenic in the Swiss Webster background (Hebert and McConnell, 2000). The *Tbx1* null mutants were at generation N5 in the Swiss Webster background. Further details are described in the Materials and methods.

We thank Dr Hanh Nguyen, Dr Vimla Aggarwal and Ms Melanie Babcock for critically reading the manuscript, intellectual advice and helpful discussions. We also thank Ms Laura Palazzolo for technical assistance. This work is supported by the American Heart Association, the March of Dimes (1-FY02-193, 1-FY2005-443) and the National Institutes of Health (DC05186-03), to B.E.M. J.S.A. is supported by a Ruth L. Kirschstein National Research Service Award (DC006977-02).

Supplementary material

Supplementary material for this article is available at http://dev.biologists.org/cgi/content/full/133/5/977/DC1

References

Abu-Issa, R., Smyth, G., Smoak, I., Yamamura, K. and Meyers, E. N. (2002). Fgf8 is required for pharyngeal arch and cardiovascular development in the mouse. *Development* **129**, 4613-4625.

Bockman, D. E. and Kirby, M. L. (1989). Neural crest function in thymus development. *Immunol. Ser.* **45**, 451-467.

Bockman, D. E., Redmond, M. E. and Kirby, M. L. (1989). Alteration of early vascular development after ablation of cranial neural crest. *Anat. Rec.* **225**, 209-217.

Bockman, D. E., Redmond, M. E. and Kirby, M. L. (1990). Altered development of pharyngeal arch vessels after neural crest ablation. *Ann. New York Acad. Sci.* **588**, 296-304.

Buckingham, M. (2001). Skeletal muscle formation in vertebrates. *Curr. Opin. Genet. Dev.* **11**, 440-448.

Burn, J. and Goodship, J. (1996). Congenital heart disease. In *Emery and Rimoin's Principles and Practice of Medical Genetics* (ed. C. J. Rimoin and D. L. Pyeritz), pp. 767-828. New York: Churchill Livingstone.

Chapman, D. L., Garvey, N., Hancock, S., Alexiou, M., Agulnik, S. I., Gibson-Brown, J. J., Cebra-Thomas, J., Bollag, R. J., Silver, L. M. and Papaioannou, V. E. (1996). Expression of the T-box family genes, Tbx1-Tbx5, during early mouse development. *Dev. Dyn.* **206**, 379-390.

Clouthier, D. E., Williams, S. C., Yanagisawa, H., Wieduwilt, M., Richardson, J. A. and Yanagisawa, M. (2000). Signaling pathways crucial for craniofacial development revealed by endothelin-A receptor-deficient mice. *Dev. Biol.* **217**, 10-24.

Couly, G. F., Coltey, P. M. and Le Douarin, N. M. (1992). The developmental fate of the cephalic mesoderm in quail-chick chimeras. *Development* **114**, 1-15.

Couly, G., Creuzet, S., Bennaceur, S., Vincent, C. and Le Douarin, N. M. (2002). Interactions between Hox-negative cephalic neural crest cells and the foregut endoderm in patterning the facial skeleton in the vertebrate head. *Development* **129**, 1061-1073.

Crump, J. G., Maves, L., Lawson, N. D., Weinstein, B. M. and Kimmel, C. B. (2004). An essential role for Fgfs in endodermal pouch formation influences later craniofacial skeletal patterning. *Development* **131**, 5703-5716.

DiGeorge, A. (1965). A new concept of the cellular basis of immunity. *J. Pediatr.* **67**, 907.

Epstein, J. A. (2000). Pax3 and vertebrate development. *Methods Mol. Biol.* **137**, 459-470.

Fekete, D. M. and Wu, D. K. (2002). Revisiting cell fate specification in the inner ear. *Curr. Opin. Neurobiol.* **12**, 35-42.

Frank, D. U., Fotheringham, L. K., Brewer, J. A., Muglia, L. J., Tristani-Firouzi, M., Capecchi, M. R. and Moon, A. M. (2002). An Fgf8 mouse mutant phenocopies human 22q11 deletion syndrome. *Development* **129**, 4591-4603.

Funke, B., Epstein, J. A., Kochilas, L. K., Lu, M. M., Pandita, R. K., Liao, J., Bauerndistel, R., Schuler, T., Schorle, H., Brown, M. C. et al. (2001). Mice overexpressing genes from the 22q11 region deleted in velo-cardio-facial syndrome/DiGeorge syndrome have middle and inner ear defects. *Hum. Mol. Genet.* **10**, 2549-2556.

Graham, A. (2003). Development of the pharyngeal arches. *Am. J. Med. Genet. A* **119**, 251-256.

Graham, A. and Smith, A. (2001). Patterning the pharyngeal arches. *BioEssays* **23**, 54-61.

Hacker, A. and Guthrie, S. (1998). A distinct developmental programme for the cranial paraxial mesoderm in the chick embryo. *Development* **125**, 3461-3472.

Hebert, J. M. and McConnell, S. K. (2000). Targeting of cre to the Foxg1 (BF-1) locus mediates loxP recombination in the telencephalon and other developing head structures. *Dev. Biol.* **222**, 296-306.

Hu, T., Yamagishi, H., Maeda, J., McAnally, J., Yamagishi, C. and Srivastava, D. (2004). Tbx1 regulates fibroblast growth factors in the anterior heart field through a reinforcing autoregulatory loop involving forkhead transcription factors. *Development* **131**, 5491-5502.

Jerome, L. A. and Papaioannou, V. E. (2001). DiGeorge syndrome phenotype in mice mutant for the T-box gene, Tbx1. *Nat. Genet.* **27**, 286-291.

Kelly, R. G. and Buckingham, M. E. (2002). The anterior heart-forming field: voyage to the arterial pole of the heart. *Trends Genet.* **18**, 210-216.

Kelly, R. G., Jerome-Majewska, L. A. and Papaioannou, V. E. (2004). The del22q11.2 candidate gene Tbx1 regulates branchiomeric myogenesis. *Hum. Mol. Genet.* **13**, 2829-2840.

Kirby, M. L. and Waldo, K. L. (1990). Role of neural crest in congenital heart disease. *Circulation* **82**, 332-340.

Kirby, M. L. and Waldo, K. L. (1995). Neural crest and cardiovascular patterning. *Circ. Res.* **77**, 211-215.

Kirby, M. L., Gale, T. F. and Stewart, D. E. (1983). Neural crest cells contribute to normal aorticopulmonary septation. *Science* **220**, 1059-1061.

Le Lievre, C. S. and Le Douarin, N. M. (1975). Mesenchymal derivatives of the neural crest: analysis of chimaeric quail and chick embryos. *J. Embryol. Exp. Morphol.* **34**, 125-154.

Lewandoski, M., Meyers, E. N. and Martin, G. R. (1997). Analysis of Fgf8 gene function in vertebrate development. *Cold Spring Harb. Symp. Quant. Biol.* **62**, 159-168.

Liao, J., Kochilas, L., Nowotschin, S., Arnold, J. S., Aggarwal, V. S., Epstein, J. A., Brown, M. C., Adams, J. and Morrow, B. E. (2004). Full spectrum of malformations in velo-cardio-facial syndrome/DiGeorge syndrome mouse models by altering Tbx1 dosage. *Hum. Mol. Genet.* **13**, 1577-1585.

Lindsay, E. A. and Baldini, A. (2001). Recovery from arterial growth delay reduces penetrance of cardiovascular defects in mice deleted for the DiGeorge syndrome region. *Hum. Mol. Genet.* **10**, 997-1002.

Macatee, T. L., Hammond, B. P., Arenkiel, B. R., Francis, L., Frank, D. U. and Moon, A. M. (2003). Ablation of specific expression domains reveals discrete functions of ectoderm- and endoderm-derived FGF8 during cardiovascular and pharyngeal development. *Development* **130**, 6361-6374.

Merscher, S., Funke, B., Epstein, J. A., Heyer, J., Puech, A., Lu, M. M., Xavier, R. J., Demay, M. B., Russell, R. G., Factor, S. et al. (2001a). TBX1 is responsible for cardiovascular defects in velo-cardio-facial/DiGeorge syndrome. *Cell* **104**, 619-629.

Meyers, E. N., Lewandoski, M. and Martin, G. R. (1998). An Fgf8 mutant allelic series generated by Cre- and Flp-mediated recombination. *Nat. Genet.* **18**, 136-141.

Momma, K., Kondo, C., Matsuoka, R. and Takao, A. (1996). Cardiac anomalies associated with a chromosome 22q11 deletion in patients with conotruncal anomaly face syndrome. *Am. J. Cardiol.* **78**, 591-594.

Noden, D. M. (1983). The embryonic origins of avian cephalic and cervical muscles and associated connective tissues. *Am. J. Anat.* **168**, 257-276.

Piotrowski, T. and Nusslein-Volhard, C. (2000). The endoderm plays an important role in patterning the segmented pharyngeal region in zebrafish (Danio rerio). *Dev. Biol.* **225**, 339-356.

Piotrowski, T., Ahn, D. G., Schilling, T. F., Nair, S., Ruvinsky, I., Geisler, R., Rauch, G. J., Haffter, P., Zon, L., I., Zhou, Y. et al. (2003). The zebrafish van gogh mutation disrupts tbx1, which is involved in the DiGeorge deletion syndrome in humans. *Development* **130**, 5043-5052.

Pirvola, U., Ylikoski, J., Trokovic, R., Hebert, J. M., McConnell, S. K. and Partanen, J. (2002). FGFR1 is required for the development of the auditory sensory epithelium. *Neuron* **35**, 671-680.

Quinlan, R., Martin, P. and Graham, A. (2004). The role of actin cables in directing the morphogenesis of the pharyngeal pouches. *Development* **131**, 593-599.

Raft, S., Nowotschin, S., Liao, J. and Morrow, B. E. (2004). Suppression of neural fate and induction of inner ear morphogenesis. *Development* **131**, 1801-1812.

Shprintzen, R. J., Goldberg, R. B., Lewin, M. L., Sidoti, E. J., Berkman, M. D., Argamaso, R. V. and Young, D. (1978). A new syndrome involving cleft palate, cardiac anomalies, typical facies, and learning disabilities: velo-cardio-facial syndrome. *Cleft Palate J.* **15**, 56-62.

Soriano, P. (1999). Generalized lacZ expression with the ROSA26 Cre reporter strain. *Nat. Genet.* **21**, 70-71.

Tao, W. and Lai, E. (1992). Telencephalon-restricted expression of BF-1, a new member of the HNF-3/fork head gene family, in the developing rat brain. *Neuron* **8**, 957-966.

Trainor, P. A., Tan, S. S. and Tam, P. P. (1994). Cranial paraxial mesoderm:

regionalisation of cell fate and impact on craniofacial development in mouse embryos. *Development* **120**, 2397-2408.
Veitch, E., Begbie, J., Schilling, T. F., Smith, M. M. and Graham, A. (1999). Pharyngeal arch patterning in the absence of neural crest. *Curr. Biol.* **9**, 1481-1484.
Vitelli, F., Morishima, M., Taddei, I., Lindsay, E. A. and Baldini, A. (2002a). Tbx1 mutation causes multiple cardiovascular defects and disrupts neural crest and cranial nerve migratory pathways. *Hum. Mol. Genet.* **11**, 915-922.
Vitelli, F., Taddei, I., Morishima, M., Meyers, E. N., Lindsay, E. A. and Baldini, A. (2002b). A genetic link between Tbx1 and fibroblast growth factor signaling. *Development* **129**, 4605-4611.
Vitelli, F., Viola, A., Morishima, M., Pramparo, T., Baldini, A. and Lindsay, E. (2003). TBX1 is required for inner ear morphogenesis. *Hum. Mol. Genet.* **12**, 2041-2048.
Xu, H., Morishima, M., Wylie, J. N., Schwartz, R. J., Bruneau, B. G., Lindsay, E. A. and Baldini, A. (2004). Tbx1 has a dual role in the morphogenesis of the cardiac outflow tract. *Development* **131**, 3217-3227.
Xu, H., Cerrato, F. and Baldini, A. (2005). Timed mutation and cell-fate mapping reveal reiterated roles of Tbx1 during embryogenesis, and a crucial function during segmentation of the pharyngeal system via regulation of endoderm expansion. *Development* **132**, 4387-4395.
Yamagishi, H., Maeda, J., Hu, T., McAnally, J., Conway, S. J., Kume, T., Meyers, E. N., Yamagishi, C. and Srivastava, D. (2003). Tbx1 is regulated by tissue-specific forkhead proteins through a common Sonic hedgehog-responsive enhancer. *Genes Dev.* **17**, 269-281.
Zhang, Z., Cerrato, F., Xu, F., Vitelli, F., Morishima, M., Vincentz, J., Ma, L., Martin, J. F., Baldini, A. and Lindsay, E. (2005). Tbx1 expression in pharyngeal arch artery development. *Development* **132**, 5307-5315.